Electrochemical and Catalytic Properties of Novel Manganese(III) Complexes with Substituted 2-(2′-Hydroxyphenyl)oxazoline Ligands − X-ray Structures of Tris[5-methyl-2-(2′-oxazolinyl)phenolato]manganese(III) and Tris[5-chloro-2-(2′-oxazolinyl)phenolato]manganese(III)

Marcel Hoogenraad,[a] Kevita Ramkisoensing,[a] Syb Gorter,[a] Willem L. Driessen,[a] Elisabeth Bouwman,[a] Jaap G. Haasnoot,[a] Jan Reedijk,*[a] Taasje Mahabiersing,[b] and František Hartl[b]

Keywords: Manganese / Spectroelectrochemistry / Cyclic voltammetry / Homogeneous catalysis / Oxidations

A series of manganese complexes of the type MnL_3 were synthesised and characterised, with HL being (substituted) 2-(2′-hydroxyphenyl)oxazoline ligands. The molecular structures of [Mn(5′-Mephox)$_3$] and [Mn(5′-Clphox)$_3$] reveal their meridional configuration with a significant Jahn–Teller distortion. The ligand substituents exert a significant influence on the redox and catalytic properties of the manganese complexes. Cyclic voltammetry experiments show that the electrochemically quasi-reversible Mn^{II}/Mn^{III} and reversible Mn^{III}/Mn^{IV} redox couples shift towards higher potentials with more electron-withdrawing substituents. The same trend applies for the oxidation of the manganese(IV) complexes. Electrolysis experiments monitored with UV/Vis and EPR spectroscopy revealed that the reduction of the manganese(III) complexes to manganese(II), and their oxidation to manganese(IV) are both chemically reversible, while subsequent oxidation of the manganese(IV) species was found to be irreversible. All complexes are active oxidation catalysts with dihydrogen peroxide as the oxidant. In the oxidation of styrene, up to 220 turnover numbers were obtained towards styrene oxide. The turnover numbers in the oxidation reactions as well as the selectivity in the oxidation of styrene and *cis*-stilbene are affected significantly by the substituents, but no clear correlation with the electrochemical properties was observed. The most striking substituent effect is the higher stability of [Mn(5′-NO_2phox)$_3$] compared to the other complexes during styrene oxidation with dihydrogen peroxide in methanol.

Introduction

The presence of manganese at the active site of a wide variety of enzymes involved in oxidation catalysis has inspired the synthesis and study of manganese complexes as structural or functional models for these enzymes.[1,2] Several of these complexes have successfully been used in bleaching reactions[2] or in (asymmetric) oxidation reactions of organic substrates.[3] In most oxidation reactions, oxidants such as *tert*-butyl hydroperoxide, sodium hypochlorite, or iodosylbenzene are used. These reagents are relatively expensive and environmentally unacceptable. There is a wide interest in the use of cleaner and cheaper oxidants like molecular oxygen or hydrogen peroxide. Coordination compounds known to use hydrogen peroxide as oxidant in oxidation are manganese complexes with 1,4,7-trimethyl-1,4,7-triazacyclononane (Me_3tacn) and derived ligands and Mn−porphyrin catalysts.[4]

The introduction of substituents on the ligands has been shown to affect various properties of the catalysts. For instance, in the Mn−Me_3tacn complexes, the presence of substituents at the nitrogen atoms at the 1-, 4-, and 7-positions in the triazacyclononane ring is essential for the catalytic activity.[2] Another example is the introduction of halogen or nitro groups on porphyrin catalysts, which resulted in a higher resistance towards oxidative degradation.[5] The higher stability probably arises from a combination of electronic effects, replacement of C−H bonds by less oxidisable carbon−halogen bonds and steric crowding to reduce intermolecular catalyst degradation. As for porphyrin complexes, the catalytic efficiency of Mn−salen complexes has been reported to improve by introduction of electron-withdrawing nitro substituents.[6] However, in Mn(salen)-catalysed asymmetric epoxidation reactions, the enantiomeric excess (*ee*) of the product was significantly lower if catalysts containing ligands with electron-withdrawing substituents were used.[3,7] In fact, the most commonly used Mn−salen catalysts contain only alkyl, or alkyl and aryl groups as substituents. The use of these complexes results in high enanti-

[a] Leiden Institute of Chemistry, Gorlaeus Laboratories, Leiden University,
P. O. Box 9502, 2300 RA Leiden, The Netherlands
Fax: (internat.) + 31-71/527-4671
E-mail: reedijk@chem.leidenuniv.nl
[b] Institute of Molecular Chemistry, University of Amsterdam, Nieuwe Achtergracht 166, 1018 WV Amsterdam, The Netherlands

  1434−1948/02/0202−0377 $ 17.50+.50/0

omeric excesses of the product, but the catalyst stability is rather low, usually resulting in turnover numbers below 40 for reactions with dihydrogen peroxide as the oxidant.[3]

The didentate ligand 2-(2′-hydroxyphenyl)oxazoline (Hphox) has, like the salen ligands, a mixed N,O donor set. It is readily accessible and more stable against hydrolysis than the salen ligands.[8] Complexes with Hphox ligands and various transition metal complexes,[9,10] including manganese(III),[1,11−13] have been shown to catalyse oxidation reactions. We now wish to report novel manganese complexes MnL_3 [with HL being substituted 2-(2′-hydroxyphenyl)oxazoline ligands, see Scheme 1], their electrochemical properties, and their use as catalysts for oxidation reactions with dihydrogen peroxide as the oxidant.

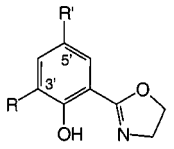

ligand	R	R′	ligand	R	R′
Hphox	H	H	H-5′-Mephox	H	CH_3
H-5′-NO_2phox	H	NO_2	H-3′-Mephox	CH_3	H
H-3′,5′-dClphox	Cl	Cl	H-5′-MeOphox	H	OCH_3
H-5′-Clphox	H	Cl			

Scheme 1. Structures of the ligands

Results and Discussion

Syntheses and Characterization of the [MnL_3] Complexes

Complexes of the type [MnL_3] were obtained by two different methods. The syntheses of [Mn(5′-Clphox)$_3$], [Mn(3′-Mephox)$_3$], [Mn(5′-Mephox)$_3$], and [Mn(5′-MeOphox)$_3$] from $Mn(OAc)_2$ and the appropriate ligand in methanol, are similar to the synthesis of [Mn(phox)$_3$].[12] The synthesis of [Mn(5′-NO_2phox)$_3$] and [Mn(3′,5′-dClphox)$_3$] was accomplished by applying the procedure used for the synthesis of [tris(8-oxyquinoline)−manganese(III)].[14] This latter method involves the addition of an ethanolic solution of the ligand to $Mn(OAc)_3$ in ethanol. In this manner, a dark brown precipitate could be isolated within a number of hours, which − after recrystallisation − afforded the desired compounds in good purity.

For all complexes, the parent peak observed in the electrospray mass spectra was the $[MnL_2]^+$ fragment. Further characterisation of the complexes was performed with IR and UV/Vis spectroscopy. The UV/Vis spectra of the complexes, except [Mn(5′-NO_2phox)$_3$], exhibit a ligand-to-metal charge transfer (LMCT) band around 370 nm and π→π* transitions of the ligand at around 310, 260, and 210 nm. No d-d transitions are observed due to the poor solubility of the complexes. The π→π* transitions are also present in the spectra of the free ligands. For [Mn(5′-NO_2phox)$_3$], two intense absorption bands at 340 and 222 nm are observed. These bands are also observed in the free ligand and can be ascribed to π→π* transitions (see the spectroelectrochemical section below). For all complexes, the manganese(III) oxidation state is confirmed by the absence of an EPR signal (at 77 K and 298 K) and by the magnetic moments at room temperature ranging from 4.10 μ_B ([Mn(3′,5′-dClphox)$_3$]) to 4.96 μ_B ([Mn(5′-MeOphox)$_3$]). These data are close to the spin-only value of 4.92 μ_B for high-spin manganese(III), the deviation being caused by orbital effects. ^{1}H NMR spectroscopy of the complexes have been used,[1,13] however, the paramagnetic ^{1}H NMR signals of these complexes could not be assigned; in order to assign the signals, systematic substitution of the hydrogen atoms is required.

Molecular Structure of [Mn(5′-Mephox)$_3$]

In the unit cell of [Mn(5′-Mephox)$_3$], with $Z = 4$, two similar, independent molecules are present. The crystallographic data are presented in Table 1.

Table 1. Crystallographic data for *mer*-[Mn(5′-Mephox)$_3$] and *mer*-[Mn(5′-Clphox)$_3$]

	[Mn(5′-Mephox)$_3$]	[Mn(5′-Clphox)$_3$]
Empirical formula	$C_{30}H_{30}MnN_3O_6$	$C_{27}H_{21}Cl_3MnN_3O_6$
Molecular mass	583.52	644.78
Crystal dimensions [mm]	0.55×0.3×0.2	0.45×0.35×0.1
Symmetry cell setting	triclinic	triclinic
Symmetry space group	P$\bar{1}$	P$\bar{1}$
a [Å]	12.725(7)	7.943(5)
b [Å]	14.299(6)	12.237(12)
c [Å]	16.16(2)	15.301(5)
α [°]	92.61(3)	68.40(3)
β [°]	107.52(3)	79.62(5)
γ [°]	105.15(3)	83.53(5)
Cell volume [Å^3]	2684(2)	1358.5(16)
Z	4	2
F(000)	1216	656
$D_{calcd.}$ [g cm^{-3}]	1.445(2)	1.576(2)
μ (Mo-K$_\alpha$) [mm^{-1}]	0.54	0.83
T [K]	77	293
R	0.058	0.039
wR	0.083	0.053
S	1.259	1.12
No residual density outside [e Å^{-3}]	−3.00, 1.45	−1.33, 0.95

A Platon[15] plot of one of the independent molecules of [Mn(5′-Mephox)$_3$] is shown in Figure 1. The molecular structure largely resembles that of [Mn(phox)$_3$],[12] having the MnN_3O_3 chromophore in a meridional configuration with a significant tetragonal distortion. The absence of

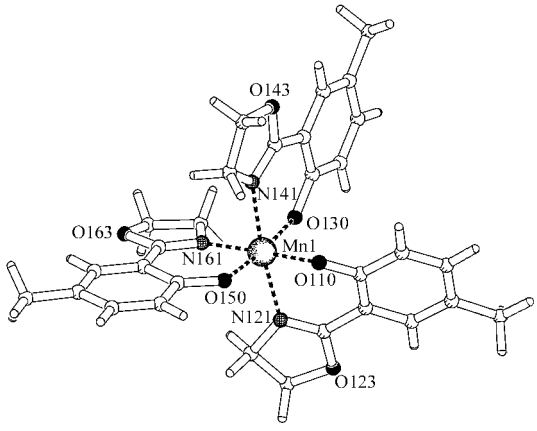

Figure 1. Platon[15] projection of one of the independent molecules of *mer*-[Mn(5′-Mephox)$_3$]

counter ions and the differences in the Mn−L bond lengths due the Jahn−Teller effect, characteristic for a d^4 configuration, confirm the manganese(III) oxidation state.

Selected bond lengths and bond angles for one [Mn(5′-Mephox)$_3$] molecule are given in Table 2. The differences in the ligand−metal bond lengths between the two independent molecules fall within 0.01 Å, while the bond angles deviate within a few degrees. The largest difference is found for the angle contained by the *trans*-O−Mn−O bonds, that expands from 173.15(18)° in one independent molecule to 177.7(2)° in the other. The structure of [Mn(5′-Mephox)$_3$] (Figure 1) has the elongated Jahn−Teller axis along the N(121)−Mn−N(141) bonds, as revealed by the long bond lengths Mn−N(121) and Mn−N(141) of 2.232(5) and 2.246(5) Å, respectively, compared to 2.033(6) Å for the Mn−N(161) bond. The Mn−O bond lengths are around 1.90 Å.

Table 2. Selected bond lengths [Å] and angles [°] of one molecule of *mer*-[Mn(5′-Mephox)$_3$] and of *mer*-[Mn(5′-Clphox)$_3$]

[a]	[Mn(5′-Mephox)$_3$]	[Mn(5′-Clphox)$_3$]
Mn1−O10	1.898(5)	1.894(4)
Mn1−O30	1.896(6)	1.927(5)
Mn1−O50	1.912(6)	1.889(4)
Mn1−N21	2.232(5)	2.238(6)
Mn1−N41	2.246(5)	2.244(5)
Mn1−N61	2.033(6)	2.033(5)
O10−Mn1−N21	84.4(2)	85.13(18)
O10−Mn1−O30	91.7(3)	91.92(18)
O10−Mn1−N41	90.4(2)	90.28(17)
O10−Mn1−O50	92.4(3)	177.57(18)
O10−Mn1−N61	177.6(2)	90.1(2)
N21−Mn1−O30	90.1(2)	90.5(2)
N21−Mn1−N41	173.8(2)	172.67(18)
N21−Mn1−O50	95.8(2)	94.19(18)
N21−Mn1−N61	93.3(2)	91.5(2)
O30−Mn1−N41	86.5(2)	84.0(2)
O30−Mn1−O50	173.15(18)	90.42(18)
O30−Mn1−N61	87.9(3)	177.57(19)
N41−Mn1−O50	87.9(2)	90.63(18)
N41−Mn1−N61	91.9(2)	94.2(2)
O50−Mn1−N61	88.3(3)	87.58(19)

[a] Due to the presence of two independent molecules in the asymmetric unit, the donor atoms for [Mn(5′-Mephox)$_3$] listed in this Table should be read as O1xx and N1xx.

Molecular Structure of [Mn(5′-Clphox)$_3$]

The crystallographic data are presented in Table 1. The unit cell, with $Z = 2$, contains the two meridional stereoisomers of the complex. Selected bond lengths and bond angles are given in Table 2. The structure of [Mn(5′-Clphox)$_3$] (Figure 2) has the elongated Jahn−Teller axis along the N21−Mn−N41 axis as shown by the long bond lengths Mn−N21 and Mn−N41 of 2.238(6) and 2.244(5) Å, respectively, compared to 2.033(5) Å for the Mn−N61 bond. The Mn−O bond lengths are around 1.90 Å. The ligand bite angle varies between 84.0(2)° and 87.58(19)° for the O30−Mn1−N41 and O10−Mn1−N21 angles, respectively.

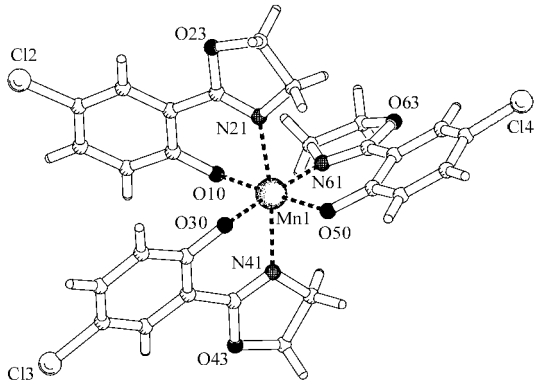

Figure 2. Platon[15] projection of *mer*-[Mn(5′-Clphox)$_3$]

As a matter of fact, all bond angles and distances for [Mn(5′-Mephox)$_3$] and [Mn(5′-Clphox)$_3$] are uneventful and very similar to those of [Mn(phox)$_3$].[12] The Mn−N bond lengths of these complexes of the type [MnL$_3$] vary from 2.033(5) to 2.060(2) Å for the equatorial Mn−N bonds and from 2.192(2) to 2.246(2) Å for the axial Mn−N bonds, while the Mn−O bond lengths are between 1.8823(17) and 1.958(2) Å.

Redox Properties of the [MnL$_3$] Complexes

Cyclic Voltammetry

The redox properties of the [MnL$_3$] complexes were investigated in acetonitrile. The potentials are given against Ag/AgCl. The investigated phox-type ligands were not redox-active between +2.00 and −2.00 V, except for H-5′-NO_2phox, which is reducible at −1.22 V (see below).

The [MnL$_3$] complexes show a (quasi)reversible one-electron cathodic wave ascribed to the reduction of manganese(III) to manganese(II), and a fully reversible one-electron anodic wave corresponding to the oxidation of manganese(III) to manganese(IV). The $E_{1/2}$ and ΔE_p values for these redox couples (Table 3) are strongly influenced by the ligand substituents.

The Mn^{III}/Mn^{IV} redox couples are fully reversible, as indicated by the peak-to-peak separations ranging from 65 to 90 mV and the i_{pc}/i_{pa} ratio of 1.[16] The linear relationship

Table 3. Electrochemical data for the oxidation and reduction of the manganese(III) centre of the [MnL$_3$] complexes

Complex[a]	Mn^{III}/Mn^{II} $E_{1/2}$	ΔE_p	Mn^{III}/Mn^{IV} $E_{1/2}$	ΔE_p
[Mn(5′-NO_2phox)$_3$]	+0.12	80	+0.87	65
[Mn(3′,5′-dClphox)$_3$]	−0.07	100	+0.75	65
[Mn(5′-Clphox)$_3$]	−0.26	120	+0.60	75
[Mn(phox)$_3$]	−0.42	260	+0.48	85
[Mn(5′-Mephox)$_3$]	−0.45	180	+0.42	60
[Mn(3′-Mephox)$_3$]	−0.52	230	+0.40	90
[Mn(5′-MeOphox)$_3$]	−0.49	220	+0.41	90

[a] In acetonitrile solutions containing 0.05 M Bu_4NPF_6 at a scan rate of 0.10 V/s; $E_{1/2}$ in V (vs. Ag/AgCl), ΔE_p in mV.

between the peak current i_{pa} and the square root of the scan rate (v) in the range of 0.2 to 2 V/s is indicative of a diffusion-controlled process.[16] The marked positive shift of both the reduction and oxidation potentials of the $[MnL_3]$ complexes with the electron-withdrawing substituents on the phox ligands closely resembles the redox properties of related mononuclear manganese(IV)[17] and manganese(III)[18,19] complexes with substituted phenolate ligands showing the same trend. For the Mn^{III}/Mn^{II} redox couples, large differences between the complexes are observed in the ΔE_p value. For the Mn−phox complexes with the electron-withdrawing substituents, the peak-to-peak separation lies between 80 and 120 mV, just slightly above the value expected for a electrochemically reversible process.[16] However, the complexes with more electron-donating ligands show much larger peak-to-peak separation, indicating quasi-reversible redox processes.

At higher potentials, yet another anodic process is observed for the formally manganese(IV) centre. The ligand substituents again exert a significant effect on the oxidation potentials (Table 4). No clear correlation exists in this case between the substituent's nature and the ΔE_p values.

Table 4. Electrochemical data for the Mn−phox complexes: electrochemically irreversible oxidations of the manganese(IV) species at higher potentials

Complex[a]	E_{pa}	E_{pc}	ΔE_p
$[Mn(5'\text{-}NO_2phox)_3]^+$	+1.59	+1.37	220
$[Mn(3',5'\text{-}dClphox)_3]^+$	+1.28	+1.14	140
$[Mn(5'\text{-}Clphox)_3]^+$	+1.31	+1.16	150
$[Mn(phox)_3]^+$	+1.30	+1.06	240
$[Mn(5'\text{-}Mephox)_3]^+$	+1.13	+0.95	180
$[Mn(3'\text{-}Mephox)_3]^+$	+1.17	+0.90	270
$[Mn(5'\text{-}MeOphox)_3]^+$	+0.98	−	−

[a] In acetonitrile solutions containing 0.05 M Bu_4NPF_6 at a scan rate of 0.10 V/s; E_{pa} and E_{pc} in V (vs. Ag/AgCl), ΔE_p in mV.

The oxidation of the manganese(IV) complexes is chemically irreversible, as evidenced by the peak-current ratios i_{pc}/i_{pa}, significantly smaller than 1 at moderate scan rates. The cyclic voltammogram of $[Mn(5'\text{-}MeOphox)_3]$ does not show any cathodic counter-peak on the reverse scan beyond the oxidation of the manganese(IV) compound.

Reduction of the formally manganese(II) species was observed, in the available potential window, only for the complexes with the most electron-withdrawing phox ligands, $[Mn(3',5'\text{-}dClphox)_3]$ and $[Mn(5'\text{-}NO_2phox)_3]$ (Figure 3). In both cases, the reduction of the manganese(II) species consumed more than one electron, as deduced from the comparison of the corresponding cathodic peak currents with those for the reversible Mn^{III}/Mn^{II} and Mn^{III}/Mn^{IV} couples. The reduction of $[Mn(5'\text{-}NO_2phox)_3]^-$ at $E_{pc} = -1.56$ V produced a species that could be further reduced at $E_{pc} = -1.81$ V. The latter cathodic step is chemically reversible, pointing to the reduction of the nitro groups on the phox ligands. The cyclic voltammogram of the uncoordinated H-5′-NO_2phox ligand shows an irreversible reduction step at $E_{pc} = -1.22$ V, followed by a quasi-reversible

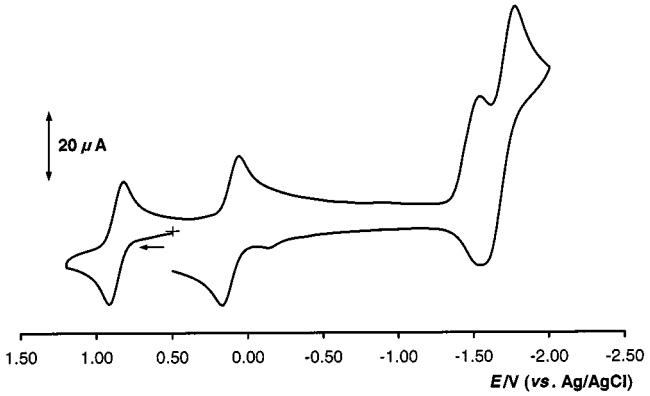

Figure 3. Cyclic voltammogram of $[Mn(5'\text{-}NO_2phox)_3]$ at a scan rate of 0.10 V/s in an acetonitrile solution containing 0.05 M Bu_4NPF_6

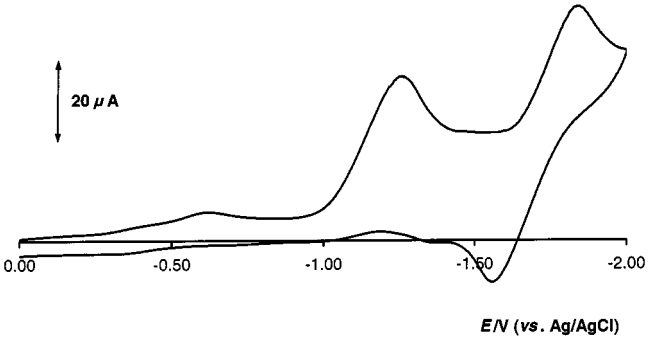

Figure 4. Cyclic voltammogram of H-5′-NO_2phox at a scan rate of 0.10 V/s in an acetonitrile solution containing 0.05 M Bu_4NPF_6

step at $E_{1/2} = -1.68$ V (Figure 4). The potential of this quasi-reversible step is nearly identical with that of the reversible cathodic process ($E_{1/2} = -1.66$ V), following the irreversible reduction of $[Mn(5'\text{-}NO_2phox)_3]^-$, suggesting that the irreversible process in the complex results in dissociation of at least one $[5'\text{-}NO_2phox]^-$ ligand. This anionic compound is obviously also produced during the irreversible reduction of H-5′-NO_2phox at $E_{pc} = -1.22$ V. Further evidence for this explanation was obtained from corresponding UV/Vis spectroelectrochemical experiments (vide infra). This behaviour is in agreement with that reported for the 4-nitro-thiophenolate anion ($[4\text{-}O_2NC_6H_4S]^-$), which can be reduced, reversibly, at the nitro group.[20] The latter cathodic process also occurred upon the reduction of the complex $[Pt^{II}(bpy^{\cdot-})(4\text{-}O_2NC_6H_4S)_2]^-$.[20] In view of these arguments, it is not surprising that the irreversible reduction of $[Mn(3',5'\text{-}dClphox)_3]^-$ at $E_{pc} = -1.86$ V is not followed by such a reversible cathodic step because further reduction of the liberated $[3',5'\text{-}dClphox]^-$ ligand is not facile. The reduction of the latter Mn^{II} complex was followed instead by a minor, irreversible wave at $E_{pc} = -2.10$ V, belonging to a secondary product that remains unassigned.

The strong dependence of the electrode potentials on the electron-withdrawing (NO_2, Cl) or electron-donating (Me, MeO) character of the phox substituents implies that the frontier molecular (redox) orbitals of the high-spin man-

ganese(III) complexes possess a significant contribution from the phox ligands. This qualitative presumption has been indeed confirmed by Extended Hückel calculations with the programme CACAO,[21] using the X-ray structure data of $[Mn(phox)_3]$. The calculated data show that the closely spaced HOMO and HOMO-1 ($\Delta E = 0.064$ eV) frontier orbitals of the complex are delocalised over the manganese(III) ion and the phox ligands. The one-electron containing HOMO possesses 69% Mn and 22% phenolate character. The singly occupied HOMO-1 has a similar character, with a slightly larger phenolate contribution (27%) and smaller Mn contribution (65%). The oxidation and reduction processes of the studied $[ML_3]$ complexes to the manganese(IV) and manganese (II) complexes, respectively, may therefore be assigned as predominantly metal-localized, although with a significant ligand influence.

UV/Vis Spectroelectrochemistry with $[Mn(phox)_3]$ and $[Mn(5'\text{-}NO_2phox)_3]$

A valuable approach in investigating the redox behaviour of the Mn−phox complexes of the type $[MnL_3]$ is to monitor the spectroscopic changes during electrolysis with methods such as UV/Vis and EPR spectroscopy. With these spectroelectrochemical methods, the chemical reversibility of the redox processes can be studied on the time scale of minutes. UV/Vis spectroelectrochemistry has been employed for mononuclear manganese complexes with nitrogen ligands[22] and mixed oxygen/nitrogen ligands.[23] To obtain more insight into the redox behaviour of $[Mn(phox)_3]$ and $[Mn(5'\text{-}NO_2phox)_3]$, the changes in their UV/Vis spectra were studied during electrolysis in acetonitrile at room temperature. The results are summarized in Table 5.

Table 5. UV/Vis absorption bands of the formally manganese(II), manganese(III), and manganese(IV) compounds, recorded in the course of the spectroelectrochemical experiments

Complex	λ_{max} (ε)[a]
$[Mn(phox)_3]^+$	216, 293 (1.2×10^4), 380 (sh), 430 (sh), 575 (4.0×10^3)
$[Mn(phox)_3]$	216, 319 (9.7×10^3), 360 (sh)
$[Mn(phox)_3]^-$	222, 349 (1.5×10^4)
$[Mn(5'\text{-}NO_2phox)_3]^+$	211, 230, 320 (4.0×10^4), 390 (sh), 582 (7.6×10^3)
$[Mn(5'\text{-}NO_2phox)_3]$	222, 358 (4.4×10^4)
$[Mn(5'\text{-}NO_2phox)_3]^-$	222, 340 (sh), 397 (6.2×10^4)

[a] In acetonitrile; λ_{max} in nm, ε in $M^{-1}\cdot cm^{-1}$; the ε values for the bands around 210−220 nm vary depending on the concentration of the complexes; sh = shoulder.

The reduction of $[Mn(phox)_3]$ at −0.55 V resulted in a colour change from green to light-brown. The most remarkable feature in the UV/Vis spectra of the manganese(II) product is the appearance of a peak at 349 nm, attributed to an LMCT transition. The π→π* transition of the ligand shifted slightly from 216 to 222 nm. Isosbestic points are observed at 381, 329, 242, and 214 nm. Reoxidation of the stable manganese(II) species at −0.29 V resulted in complete reappearance of the initial UV/Vis spectrum of $[Mn(phox)_3]$.

The reduction of $[Mn(5'\text{-}NO_2phox)_3]$ at +0.08 V resulted in a yellow solution. In the UV/Vis spectra, the shift of the absorption peak at 358 nm to 397 nm is attributed to changes in the intense π→π* transition of the nitro group (Figure 5).

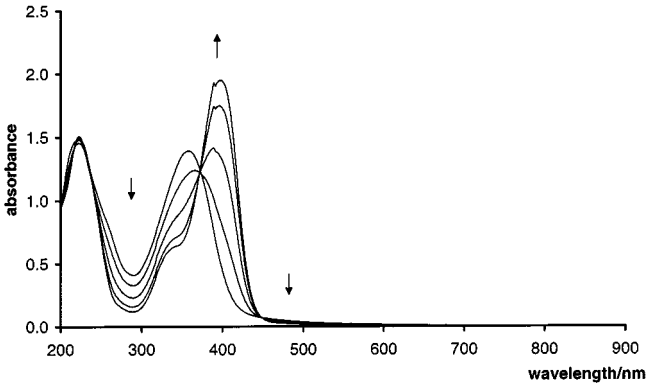

Figure 5. UV/Vis spectroscopic changes recorded during the electrochemical reduction of $[Mn(5'\text{-}NO_2phox)_3]$ from manganese(III) to manganese(II)

The peak at 222 nm, ascribed to the aromatic π→π* transition, hardly changes. Two isosbestic points occur at 372 and 449 nm. The presence of the π→π*(NO_2) absorption band makes it difficult to compare the spectra of the manganese(II) complexes $[Mn(5'\text{-}NO_2phox)_3]^-$ and $[Mn(phox)_3]^-$. However, the shoulder in the spectrum of the manganese(II) species at 340 nm has presumably the same origin as the peak at 349 nm in the UV/Vis spectrum of $[Mn(phox)_3]^-$. This observation is important, because it indicates that one-electron-reduced $[Mn(phox)_3]^-$ and $[Mn(5'\text{-}NO_2phox)_3]^-$ are electronically similar. Both anionic complexes are also inherently stable.

Cyclic voltammetry revealed that the anionic complexes $[Mn(3',5'\text{-}dClphox)_3]^-$ and $[Mn(5'\text{-}NO_2phox)_3]^-$ undergo irreversible reduction that may result in dissociation of one or more anionic phox ligands (see previous section). This assumption could be confirmed by UV/Vis spectroelectrochemistry. The UV/Vis spectra recorded during the reduction of $[Mn(5'\text{-}NO_2phox)_3]^-$ at −1.56 V exhibit isosbestic points at 483, 408, and 207 nm and a shift of the intense absorption band due to the π→π*(NO_2) transition from 397 nm to 426 nm (Figure 6).

Importantly, the UV/Vis spectrum of the product (absorption maxima at 426, 330 and 228 nm) is identical with that of $[5'\text{-}NO_2phox]^-$ recorded after the one-electron reduction of H-5′-NO_2phox (Figure 6, inset). This result implies that the irreversible reduction of $[Mn(5'\text{-}NO_2phox)_3]^-$ indeed affords the uncoordinated $[5'\text{-}NO_2phox]^-$ ligand, which dissociates due to the decreased positive charge on the manganese centre in the primarily $Mn^{II}\rightarrow Mn^{I}$ electron-transfer step. The liberated anion $[5'\text{-}NO_2phox]^-$ is further reversibly reduced at the NO_2 group at $E_{1/2} = -1.66$ V, resulting in the formation of $[5'\text{-}NO_2phox]^{2-}$. As expected, the latter reduction process increases the energy of the

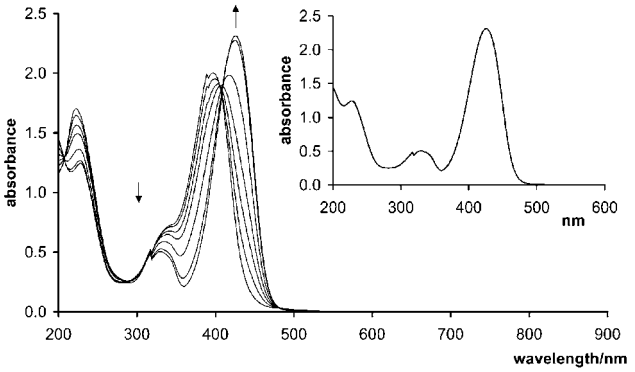

Figure 6. UV/Vis spectroscopic changes recorded during the in situ irreversible reduction of $[Mn(5'\text{-}NO_2phox)_3]^-$; inset: UV/Vis spectrum of $[5'\text{-}NO_2phox]^-$ formed during the irreversible reduction of $[H\text{-}5'\text{-}NO_2phox]^-$

$\pi\rightarrow\pi^*(NO_2)$ electronic transition[20] and the corresponding absorption band shifts from 426 nm for $[5'\text{-}NO_2phox]^-$ to 291 nm for $[5'\text{-}NO_2phox]^{2-}$.

The oxidation of the Mn−phox complexes to the manganese(IV) species is fully reversible according to cyclic voltammetry. The spectroelectrochemical experiments show that this also applies for the time scale of minutes. In the UV/Vis spectra recorded during the stepwise electrolytic oxidation of $[Mn(5'\text{-}NO_2phox)_3]$ at 0.90 V, two isosbestic points are observed at 331 and 408 nm (Figure 7).

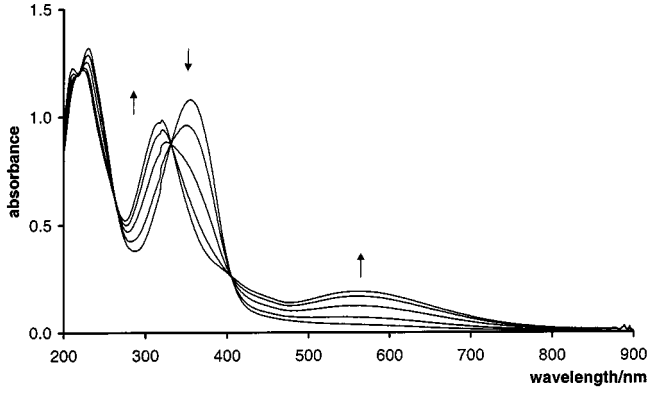

Figure 7. UV/Vis spectroscopic changes recorded during the electrochemical oxidation of $[Mn(5'\text{-}NO_2phox)_3]$ from manganese(III) to manganese(IV)

The most important feature in the UV/Vis spectrum of the manganese(IV) complex is the new broad absorption band at 582 nm; based on its intensity, it can be assigned to an LMCT transition. This visible absorption results in the dark blue colour of the complex, also known for some other manganese(IV) complexes.[24,25] The $\pi\rightarrow\pi^*(NO_2)$ transition shifts from 358 to 320 nm. Further oxidation of $[Mn(5'\text{-}NO_2phox)_3]^+$ at +1.59 V led to irreversible disappearance of the LMCT band and degradation of the complex.

UV/Vis spectra collected during the stepwise oxidation of $[Mn(phox)_3]$ at +0.52 V, show new absorption maxima at 575 and 293 nm. Isosbestic points are present at 371, 332 and 277 nm. The new broad peak at 575 nm corresponds to that at 582 nm in the UV/Vis spectrum of the dark blue $[Mn(5'\text{-}NO_2phox)_3]^+$ complex, indicating that similar complexes are formed. The $[Mn(phox)_3]^+$ compound shows a small oxidation wave at +1.30 V. The UV/Vis spectra taken during this anodic step reveal a new absorption band at 424 nm and isosbestic points at 470 and 371 nm, while all other UV/Vis bands are diminished. Continued anodic scan shows a large wave at +1.72 V, with a peak current of approximately three times the intensity compared to the reversible one-electron oxidation of manganese(III) to manganese(IV). Similar to the oxidation of $[Mn(5'\text{-}NO_2phox)_3]^+$, irreversible disappearance of all UV/Vis absorption bands indicate oxidative degradation of the phox derivative.

EPR Spectroelectrochemistry with $[Mn(phox)_3]$ and $[Mn(5'\text{-}NO_2phox)_3]$

The UV/Vis spectroelectrochemical experiments prove that the manganese(II) and manganese(IV) complexes were stable on a time scale of several minutes. For EPR spectroelectrochemistry butyronitrile was used due to fairly good solubility of the complexes in this solvent, particularly at low temperatures. As no EPR signals of the starting complexes or their reduced or oxidized forms were observed at 223 K, EPR spectroelectrochemical experiments were performed at 77 K in a solid matrix of the frozen solutions that had first been subjected to bulk electrolysis at the E_{pa} or E_{pc} values of the precursor manganese(III) compounds upon the UV/Vis spectroscopic control (see Figures 5 and 7). The EPR spectra of the stable manganese(II) complexes show a typical six-line hyperfine signal due to coupling of the electron spin with the nuclear spin of ^{55}Mn ($I = 5/2$).[26] The EPR signals of both $[Mn(5'\text{-}NO_2phox)_3]^-$ and $[Mn(phox)_3]^-$ occur at $g = 2.00$ with $a_{Mn} = 9.0$ mT.

At 77 K, no EPR signals were observed for the oxidized manganese(IV) products $[Mn(phox)_3]^+$ and $[Mn(5'\text{-}NO_2phox)_3]^+$, even though spectra are commonly observed for other manganese(IV) complexes.[26] Their absence in this case cannot be readily explained. The cyclovoltammetric and UV/Vis spectroelectrochemical data nevertheless reveal that oxidation of $[Mn(phox)_3]$ and $Mn(5'\text{-}NO_2phox)_3]$ results in the formation of stable isostructural manganese(IV) complexes, so relaxation phenomena are likely responsible for this observation.

Catalytic Studies with the $[ML_3]$ Complexes

Oxidation of Styrene

The effect of the ligand substituents on the catalytic activity of the studied complexes $[MnL_3]$ was investigated for the oxidation of styrene in methanol at room temperature, as well as in acetone at 0 °C. The successful use of acetone as a solvent at 0 °C has been reported for oxidations with dihydrogen peroxide catalysed by Mn−Me_3tacn complexes.[27] Such reaction conditions also proved to be very suitable for the Mn−phox-catalysed oxidations. The catalytic efficiency for the different $[MnL_3]$ complexes, ex-

Table 6. Turnover numbers in the oxidation of styrene with dihydrogen peroxide in methanol or acetone catalysed by Mn−phox complexes

Catalyst	Methanol[a] Styrene oxide	Benzaldehyde	Acetone[b] Styrene oxide	Benzaldehyde	Diol[c]
[Mn(5′-NO_2phox)$_3$]	34[d]	2	207	5	18
[Mn(3′,5′-dClphox)$_3$]	23	2	108	4	5
[Mn(5′-Clphox)$_3$]	27	2	192	4	12
[Mn(phox)$_3$]	34	2	220	5	11
[Mn(5′-Mephox)$_3$]	24	2	181	4	9
[Mn(3′-Mephox)$_3$]	27	2	80	3	3
[Mn(5′-MeOphox)$_3$]	5	2	76	2	5

[a] Reactions were carried out under standard conditions: 14 μmol of the indicated Mn−phox complex was dissolved, with stirring, in 20 mL of methanol at room temperature. Subsequently, 14 mmol of substrate, 2.0 mmol of 1-MeIm, and 21 mmol of dihydrogen peroxide were added (t = 0); turnover numbers are the total turnover numbers obtained at t = 15 min. [b] Reactions were carried out under standard conditions: 10 mL of acetone and 21 mmol of dihydrogen peroxide were stirred at 0 °C for 30 min. Subsequently, 14 mmol of substrate, 2.0 mmol of 1-MeIm, and 14 μmol of the indicated Mn−phox complex were added (t = 0); turnover numbers are the total turnover numbers obtained at t = 15 min. [c] 1-Phenyl-1,2-ethanediol. [d] 72, 3, and 2 turnover numbers towards styrene oxide, benzaldehyde, and 1-phenyl-1,2-ethanediol, respectively, as determined at t = 120 min (end of the reaction).

Table 7. Turnover numbers and *cis*/*trans* ratios of the products in the oxidation of *cis*-stilbene by Mn−phox complexes with dihydrogen peroxide

Complex[a]	*cis*-Oxide	*trans*-Oxide	Benzaldehyde	Ratio *cis*/*trans*
[Mn(5′-NO_2phox)$_3$]	32	64	2	1:2.0
[Mn(3′,5′-dClphox)$_3$]	22	37	2	1:1.7
[Mn(5′-Clphox)$_3$]	18	50	2	1:2.8
[Mn(phox)$_3$]	17	50	2	1:2.9
[Mn(5′-Mephox)$_3$]	13	46	1	1:3.5
[Mn(3′-Mephox)$_3$]	9	31	2	1:3.4
[Mn(5′-MeOphox)$_3$]	4	19	1	1:4.8

[a] Reactions were carried out by stirring 10 mL of acetone and 21 mmol of H_2O_2 at 0 °C: after 30 min, subsequently 5.0 mmol of the substrate, 2.0 mmol of 1-methylimidazole, and 14 μmol of the complex were added (t = 0); turnover numbers are the total turnover numbers obtained at t = 15 min.

pressed in turnover numbers, is listed in Table 6. All reactions were performed in the presence of 2.0 mmol of 1-methylimidazole (1-Meim). An alkaline additive is required for reactions with manganese catalysts and H_2O_2; it is thought that the additive might act as a base and as an axial ligand.[12]

Small amounts of the side product benzaldehyde were obtained in all reactions. For the reactions in acetone, 1-phenyl-1,2-ethanediol was also detected as a side product. The turnover numbers towards the main product, styrene oxide, are significantly influenced by the substituents on the ligands in the [MnL_3] complexes. For the reactions in methanol, all Mn−phox complexes gave turnover numbers towards styrene oxide between 23 and 34 after 15 min, which represents an efficiency of approximately 2% relative to dihydrogen peroxide. The results in acetone show a dramatic increase in turnover numbers compared to the reactions in methanol. The efficiency relative to the oxidant increased simultaneously, varying from 5 to 15%.

In both solvents, [Mn(phox)$_3$] and [Mn(5′-NO_2phox)$_3$] show the highest efficiency. The use of Mn−phox complexes with more electron-donating ligands resulted in a significant decrease in efficiency compared to [Mn(phox)$_3$], while the use of complexes with electron-withdrawing ligands only resulted in a slightly lower efficiency. The turnover numbers obtained with the least efficient Mn−phox catalyst, [Mn(5′-MeOphox)$_3$], are relatively more enhanced in acetone compared to methanol. For the reactions in acetone, the influence of the presence of a substituent at the 3′-position is more pronounced compared to the reactions in methanol. The complexes with such ligands, [Mn(3′,5′-dClphox)$_3$] and [Mn(3′-Mephox)$_3$], exhibited much lower efficiency compared to complexes with a substituent at the 5′-position only.

Oxidation of Stilbene

In oxidation reactions of *cis*-alkenes catalysed by manganese complexes, such as Mn−salen,[7] isomerisation can occur, resulting in both *cis*- and *trans*-epoxides. For the Mn−salen complexes, this effect has been studied in detail. It has been found that the *cis*/*trans* ratio is mainly influenced by the reaction conditions,[28] the oxidant,[28,29] and the substituents on the ligand.[6,30] The oxidation of *cis*-stilbene with Mn−phox complexes results in both *cis*- and *trans*-stilbene oxide. Oxidation of *cis*-stilbene was performed with all studied [MnL_3] complexes (Table 7).

In all described reactions more *trans*- than *cis*-stilbene oxide was formed, together with small amounts of the cleavage product benzaldehyde. The ligand substituents clearly

affected the *cis*/*trans* ratio of the stilbene oxides, the complexes with electron-withdrawing ligands produced a larger amount of *cis*-stilbene oxide, while the reaction with [Mn(5′-MeOphox)$_3$] resulted in the largest relative fraction of *trans*-stilbene oxide.

The catalytic activity of the unsubstituted precursor catalyst [Mn(phox)$_3$] under similar reaction conditions for the oxidation of *trans*-stilbene and cyclohexene was also studied. Oxidation of *trans*-stilbene resulted in a TON of 49 towards the *trans*-stilbene epoxide and a TON of 3 towards the by-product benzaldehyde. Oxidation of cyclohexene with [Mn(phox)$_3$] gave a TON of 98 towards the epoxide, and additionally the allylic oxidation products were formed with a TON of 28.

Catalyst Stability

In both methanol and acetone, the catalytic reactions with most of the Mn−phox complexes were very fast during the first few minutes, and no clear differences in the reaction rates were found. After 15 min, no catalytic activity could be observed. The only exception is the [Mn(5′-NO$_2$phox)$_3$] catalyst, which remained active for up to 1 h. For [Mn(phox)$_3$] and [Mn(5′-NO$_2$phox)$_3$], the total turnover numbers to styrene oxide in time is depicted in Figure 8.

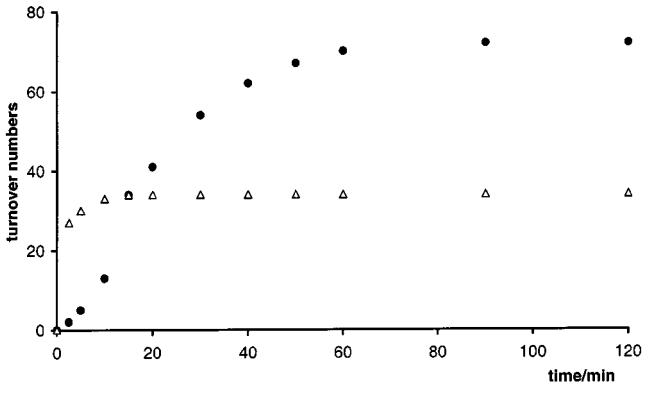

Figure 8. Oxidation of styrene with dihydrogen peroxide in methanol: cumulative turnover number in time towards styrene oxide; • = [Mn(5′-NO$_2$phox)$_3$] as catalyst; Δ = [Mn(phox)$_3$] as catalyst

The oxidation reaction with [Mn(phox)$_3$] was initially very fast, but the activity quickly diminished, with a concomitant loss of colour. In contrast, a significantly slower colour change was observed for the [Mn(5′-NO$_2$phox)$_3$]-catalysed reaction. The oxidation with this catalyst had a short induction period. Catalytic activity persisted for 1 h, resulting in a total turnover number of 72 towards styrene oxide. With both catalysts, benzaldehyde was formed in the first minutes of the reaction, while 1-phenyl-1,2-ethanediol was formed in a gradually increasing amount.

Concluding Remarks

A series of novel, readily available manganese complexes of the type [MnL$_3$] with phenol-substituted 2-(2′-hydroxyphenyl)oxazoline ligands have been synthesized. The complexes are nearly isostructural, as evidenced by the results from X-ray crystallographic studies of [Mn(phox)$_3$],[12] [Mn(5′-Mephox)$_3$] and [Mn(5′-Clphox)$_3$].

The substituents on the phenolate ring of the ligands influence the redox properties of the complexes. The electrochemically quasi-reversible Mn^{II}/Mn^{III} and reversible Mn^{III}/Mn^{IV} redox couples sensitively shifted towards higher potentials with more electron-withdrawing substituents. The same trend applies for the irreversible oxidation of the manganese(IV) complexes. (Spectro)electrochemical studies show that the manganese centre could coordinate all three anionic phox ligands in the formal oxidation states Mn^{II}, Mn^{III}, and Mn^{IV} without any pronounced change of the complex structure. The UV/Vis spectra document that reoxidation of the manganese(II) product and the back-reduction of the manganese(IV) species led to the recovery of the parent [MnL$_3$] species, proving that these redox processes are chemically reversible. In contrast to this stability, oxidation of manganese(IV) or reduction of manganese(II) resulted in decomposition, in the latter case involving the dissociation of at least one anionic [5′-NO$_2$phox]$^-$ ligand. The dissociation of the anionic phox ligand(s) probably also takes place during the reduction of [Mn(3′,5′-dClphox)$_3$]$^-$. The other formally manganese(II) anionic complexes were reduced at significantly more negative potentials and the corresponding cathodic waves were not observed within the available potential window. Ligand dissociation during the reduction of the manganese(II) complexes is not surprising, as the manganese(I) ion is hardly capable of coordinating exclusively strong σ- and π-donors, such as the anionic phox ligands.

The Mn−phox complexes are all active catalysts for the oxidation of styrene and *cis*- and *trans*-stilbene with dihydrogen peroxide as the oxidant. The substituents on the phenolate ring of the ligands significantly influenced the turnover numbers and selectivities in the oxidation reactions. The effect of the ligand substituents on the turnover numbers is roughly similar in acetone and methanol. However, considerably higher turnover numbers were obtained for styrene oxidation in acetone than in methanol, resulting in a turnover number of up to 220 towards styrene oxide with [Mn(phox)$_3$] as the catalyst, which also corresponds to increased efficiency towards dihydrogen peroxide from 2 to 15%. Although a clear general pattern can be noticed, exact correlation between the redox properties of the complexes and the turnover numbers and selectivities obtained in oxidation catalysis could not be found. This variation was probably caused by the effects that the ligands have on various reactions in solution, such as equilibria between different complexes in solution, dihydrogen peroxide decomposition and oxidation of the substrate.

The most remarkable substituent effect, the higher stability against oxidative degradation of the Mn−phox complex with the most electron-withdrawing substituents, [Mn(5′-NO$_2$phox)$_3$], was observed both in the electrochemical experiments and in oxidation catalysis. Further studies

on stability and decomposition will be published elsewhere.[31]

Experimental Section

General Remarks: The ligands were synthesised according to the synthesis for Hphox.[8] The synthesis of $[Mn(phox)_3]$ has been published before.[12] Solvents of technical grade, p.a. grade, or, for acetonitrile (Rathburn), HPLC grade quality were used as received. All p.a. grade solvents were purchased from Baker, except for acetone (Acros). Deuterated solvents for NMR measurements were obtained from Euriso-top ($CDCl_3$ and $[D_6]$DMSO) or Cambridge Isotope Laboratories, Inc. (CD_3OD). The following materials were supplied by Merck: Na_2SO_4, ferrocene, $Mn(OAc)_2{\cdot}4H_2O$, 2-aminoethanol, dihydrogen peroxide (35% in water), styrene, benzyl alcohol, and benzaldehyde. All other chemicals used were purchased from Acros.

Ligands

H-5′-NO_2phox: Starting from 15.35 g (78 mmol) of methyl 5-nitrosalicylate: Yield 7.21 g (35 mmol, 45%) of a yellow powder. ^{1}H NMR ($[D_6]$DMSO): δ = 4.17 (t, 2 H, NCH_2), 4.53 (t, 2 H, OCH_2), 7.07 (d, 1 H, H3′), 8.25 (dd, 1 H, H4′), 8.58 (d, 1 H, H6′), 13.1 (br, 1 H, OH). ^{13}C NMR ($[D_6]$DMSO): δ =52.0 (C4), 68.2 (C5), 109.4 (C1′), 118.5 (C3′), 124.3 (C5′), 128.9 (C6′), 138.1 (C4′), 164.9 (C2′), 165.9 (C2).

H-3′,5′-dClphox: Starting from 18.23 g (82 mmol) of methyl 3,5-dichlorosalicylate: Yield 16.35 g (70 mmol, 85%) of a pale yellow solid. ^{1}H NMR ($CDCl_3$): δ = 4.13 (t, 2 H, NCH_2), 4.47 (t, 2 H, OCH_2), 7.43 (d, 1 H, H6′), 7.52 (d, 1 H, H4′), 12.6 (br, 1 H, OH). ^{13}C NMR ($CDCl_3$): δ =53.3 (C4), 67.4 (C5), 112.3 (C1′), 122.4 (C3′), 122.9 (C5′), 126.0 (C6′), 132.9 (C4′), 154.6 (C2′), 165.1 (C2).

H-5′-Clphox: Starting from 10.69 g (58 mmol) of methyl 5-chlorosalicylate: Yield 7.40 (38 mmol, 66%) of a pale pink solid. ^{1}H NMR ($[D_6]$DMSO): δ = 4.07 (t, 2 H, NCH_2), 4.48 (t, 2 H, OCH_2), 7.02 (d, 1 H, H3′), 7.49 (m, 2 H, CH4′, H6′), 12.28 (s, 1 H, OH). ^{13}C NMR (D_6[DMSO]): δ =53.0 (C4), 67.3 (C5), 111.3 (C1′), 118.3 (C4′), 122.2 (C5′), 126.6 (C6′), 133.1 (C4′), 157.8 (C2′), 164.3 (C2).

H-5′-Mephox: Starting from 7.83 g (47 mmol) of methyl 5-methylsalicylate: Yield 6.18 g (35 mmol, 74%) of a pale pink solid. ^{1}H NMR ($CDCl_3$): δ = 2.23 (s, 3 H, CH_3), 4.02 (t, 2 H, NCH_2), 4.37 (t, 2 H, OCH_2), 6.79 (d, 1 H, H4′), 7.14 (d, 1 H, H3′), 7.39 (s, 1 H, H6′). ^{13}C NMR ($CDCl_3$): δ =20.3 (CH_3), 53.4 (C4), 66.6 (C5), 110.2 (C1′), 116.4 (C3′), 127.6 (C5′), 127.8 (C6′), 134.0 (C4′), 157.6 (C2′), 166.1 (C2).

H-3′-Mephox: Starting from 7.18 g (55 mmol) of ethyl 3-methylsalicylate: Yield 6.23 g (35 mmol, 88%) of a pale pink solid. ^{1}H NMR ($CDCl_3$): δ = 2.27 (s, 3 H, CH_3), 4.02 (t, 2 H, NCH_2), 4.35 (t, 2 H, OCH_2), 6.75 (t, 1 H, H5′), 7.20 (d, 1 H, H4′), 7.47 (d, 1 H, H6′). ^{13}C NMR ($CDCl_3$): δ =15.9 (CH_3), 53.4 (C4), 66.7 (C5), 110.0 (C1′), 118.0 (C5′), 125.5 (C6′), 125.7 (C3′), 134.1 (C4′), 158.1 (C2′), 166.5 (C2).

H-5′-MeOphox: Starting from 8.92 g (49 mmol) of methyl 5-methoxysalicylate: Yield 3.50 g (18 mmol, 37%) of a pale pink solid. ^{1}H NMR (CD_3OD): δ = 3.72 (s, 3 H, $ArOCH_3$), 4.05 (t, 2 H, NCH_2), 4.41 (t, 2 H, OCH_2), 6.84 (d, 1 H, H3′), 6.96 (dd, 1 H, H4′), 7.12 (d, 1 H, H6′). ^{13}C NMR (CD_3OD): δ =54.5 (C4), 56.4 ($ArOCH_3$), 68.2 (C5), 111.6 (C1′), 112.3 (C6′), 118.4 (C3′), 121.7 (C4′), 153.2 (C2′), 154.8 (C5′), 166.9 (C2).

General Synthetic Procedure for the Complexes $[Mn(5'\text{-}NO_2phox)_3]$ and $[Mn(3',5'\text{-}dClphox)_3]$: The appropriate ligand (3.0 mmol), dissolved in 10 mL of ethanol, was added to a solution of $Mn(OAc)_3{\cdot}2H_2O$ (0.27 g, 1.0 mmol) in 10 mL of ethanol. The product slowly precipitated as a black solid. Recrystallisation from ethanol afforded a black crystalline product.

$[Mn(5'\text{-}NO_2phox)_3]$: Yield 0.51 g (0.75 mmol, 75%). IR: $\tilde{\nu}$ = 1622 (s), 1312 (s), 1121 (m), 1058 (m), 871 (m), 838 (m), 714 cm^{-1} (m). $C_{27}H_{21}MnN_6O_{12}$: calcd. C 47.94, H 3.13, N 12.42; found C 47.68, H 3.37, N 12.12. ES-MS: *m*/*z*: 468 $[Mn(5'\text{-}NO_2phox)_2]^+$, 209 [H-5′-$NO_2$phox + H^+]. μ_{eff} = 4.87 μ_B (at 22.5 °C).

$[Mn(3',5'\text{-}dClphox)_3]$: Yield 0.51 g (0.68 mmol, 68%). IR: $\tilde{\nu}$ = 1617 (s), 1582 (m), 1437 (s), 1418 (s), 1370 (m), 1308 (m), 1234 (s), 1194 (m), 954 (m), 872 (m), 784 (s), 751 (m), 738 cm^{-1} (m). $C_{27}H_{18}Cl_6MnN_3O_6$: calcd. C 43.35, H 2.43, N 5.62; found C 43.08, H 2.45, N 5.31. ES-MS: *m*/*z*: 519, 517, 515 $[Mn(3',5'\text{-}dClphox)_2]^+$, 234, 232 [H-3′,5′-dClphox + H^+]. μ_{eff} = 4.10 μ_B (at 22.5 °C).

$[Mn(5'\text{-}Clphox)_3]$: To a solution of $Mn(OAc)_2{\cdot}4H_2O$ (0.25 g, 1.0 mmol) in 20 mL of MeOH was added 0.59 g (3.0 mmol) of H-5′-Clphox. After the addition of 10 mL of diethyl ether, the ligand dissolved and within several minutes the solution turned dark green. The dark green complex precipitated within 1 d. Recrystallisation from ethanol afforded X-ray quality crystals. Yield 0.52 g (0.81 mmol, 81%). IR: $\tilde{\nu}$ = 1622 (s), 1458 (s), 1405 (m), 1314 (s), 1237 (s), 1224 (s), 1100 (m), 1055 (m), 941 (m), 827 (m), 820 (m), 728 cm^{-1} (m). $C_{27}H_{21}Cl_3MnN_3O_6$: calcd. C 50.30, H 3.28, N 6.52; found C 50.41, H 3.30, N 6.33. ES-MS: *m*/*z*: 449, 447 $[Mn(5'\text{-}Clphox)_2]^+$, 200, 198, [H-5′-Clphox + H^+]. μ_{eff} = 4.74 μ_B (at 22.5 °C).

General Synthetic Procedure for $[Mn(3'\text{-}Mephox)_3]$, $[Mn(5'\text{-}Mephox)_3]$ and $[Mn(5'\text{-}MeOphox)_3]$: A solution of the ligand (3.0 mmol) and 0.30 g (3.0 mmol) of triethylamine in 10 mL of methanol was added to a solution of $Mn(OAc)_2{\cdot}4H_2O$ (0.25 g, 1.0 mmol) in 10 mL of methanol. The solution turned dark green immediately and within a number of days the complex precipitated. The complexes were recrystallised from methanol/water (2:1) ($[Mn(3'\text{-}Mephox)_3]$ and $[Mn(5'\text{-}MeOphox)_3]$) or ethanol ($[Mn(5'\text{-}Mephox)_3]$).

$[Mn(5'\text{-}Mephox)_3]$: Yield 0.43 g (0.72 mmol, 72%). X-ray quality crystals were obtained after recrystallisation from methanol. IR: $\tilde{\nu}$ = 1626 (s), 1601 (m), 1552 (m), 1485 (m), 1472 (s), 1323 (s), 1257 (m), 1242 (s), 1233 (s), 1201 (m), 1074 (m), 1057 (s), 866 (m), 826 (m), 792 cm^{-1} (m). $C_{30}H_{30}MnN_3O_6$: calcd. C 61.75, H 5.18, N 7.20; found C 61.53, H 5.32, N 7.30. ES-MS: *m*/*z*: 583 $[Mn(5'\text{-}Mephox)_3]^+$, 407 $[Mn(5'\text{-}Mephox)_2]^+$, 178 [H-5′-Mephox + H^+]. μ_{eff} = 4.47 μ_B (at 22.5 °C).

$[Mn(3'\text{-}Mephox)_3]$: Yield 0.45 g (0.77 mmol, 77%). IR: $\tilde{\nu}$ = 1622 (s), 1561 (m), 1424 (s), 1394 (m), 1382 (m), 1322 (m), 1252 (m), 1239 (s), 1136 (m), 1088 (m), 955 (m), 863 (m), 748 cm^{-1} (m). $C_{30}H_{30}MnN_3O_6$: calcd. C 61.75, H 5.18, N 7.20; found C 61.33, H 5.05, N 7.14. ES-MS: *m*/*z*: 407 $[Mn(3'\text{-}Mephox)_2]^+$, 17[H-3′-Mephox + H^+]. μ_{eff} = 4.82 μ_B (at 22.5 °C).

$[Mn(5'\text{-}MeOphox)_3]$: Yield 0.50 g (0.79 mmol, 79%). IR: $\tilde{\nu}$ = 1633 (m), 1601 (s), 1558 (m), 1471 (s), 1416 (m), 1273 (m), 1242 (m), 1206 (s), 1184 (m), 1040 (m), 815 (m), 794 cm^{-1} (m). $C_{30}H_{30}MnN_3O_9$: calcd. C 57.06, H 4.79, N 6.65; found C 57.10, H 4.73, N 6.65. ES-MS: *m*/*z*: 631 $[Mn(5'\text{-}MeOphox)_3]^+$, 439 $[Mn(5'\text{-}MeOphox)_2]^+$. μ_{eff} = 4.96 μ_B (at 22.5 °C).

X-ray Crystallographic Study: The data were collected with an Enraf−Nonius CAD-4 diffractometer with graphite-monochromated Mo-K_α radiation (λ = 0.71073 Å) and ω-2θ scan. The cell dimensions were determined by 24 independent reflections. The data were corrected for linear decay, but not for absorption effects. Atomic scattering factors and anomalous dispersion constants were taken from the International Tables for X-ray Crystallography.[32] For both compounds the positions of the heavy atoms were determined from Patterson maps (DIRDIF).[33] The remainder of the non-hydrogen atoms were found in subsequent ΔF syntheses (XTAL).[34] Hydrogen atoms were placed at calculated positions and were not included in refinement. Full-matrix least-squares refinement (XTAL)[34] on F of the positional and the anisotropic thermal parameters of the non-hydrogen atoms. The hydrogen atoms, with fixed isotropic thermal parameters, were included, riding on a fixed distance of their parent atoms. Crystallographic data (excluding structure factors) for the structures reported in this paper have been deposited with the Cambridge Crystallographic Data Centre as supplementary publications no. CCDC-144587 [Mn(5′-Mephox)$_3$] and -144588 [Mn(5′-Clphox)$_3$]. Copies of the data can be obtained free of charge on application to CCDC, 12 Union Road, Cambridge CB2 1EZ, UK [Fax: (internat.) + 44-1223/336-033; E-mail: deposit@ccdc.cam.ac.uk].

Equipment: IR spectra were recorded with a Perkin−Elmer FT-IR Paragon 1000 spectrometer. Samples were measured as KBr pellets. ^{1}H and ^{13}C NMR (^{1}H decoupled) spectra of the ligands were recorded with Jeol JNM-FX 200 or Bruker 300 DPX MHz spectrometers. ^{1}H NMR spectra of the complexes (up to 0.2 mM) were recorded with a Bruker 300 DPX MHz spectrometer. These spectra were collected using an inversion recovery pulse sequence π-τ-π/2. The value of τ (12 or 13 ms) was chosen such that the paramagnetic signals were relaxed, while the signals from the diamagnetic compounds in solution remained inverted. Other operating parameters were as follows: spectrometer frequency 300.13 Hz; data block size (SI) 32 K; acquisition time 200 ms; line broadening 5 Hz; window 30 kHz. Elemental analyses were carried out by the Microanalytical Laboratory, University College Dublin or at Leiden University with a Perkin−Elmer series II CHNS/O analyser 2400. A Johnson Matthey Alfa Products Mk1 magnetic susceptibility balance was used to determine the magnetic moments of the powdered complexes at room temperature. Standard electrospray mass spectra of the complexes were recorded with a Finnigan MAT TSQ-70 mass spectrometer, equipped with an electrospray interface (ESI). The spectra were collected by constant infusion of the analyte, dissolved in a methanol/water (80:20) mixture containing 1% acetic acid. A Varian Star 3400CX gas chromatograph with a J&W Scientific/Fisons DB-1701 (14% cyanopropylphenyl-methylpolysiloxane) column was used for analysis of the oxidation experiments. The turnover numbers given are the total turnover numbers per manganese ion after the indicated period of time. All reactions were performed at least in duplicate.

Cyclic Voltammetry: The cyclic voltammetry measurements were performed with an Autolab PGstat10 potentiostat controlled by the GPES4 software. A three-electrode system was used, consisting of a glassy carbon (GC) working electrode, a platinum (Pt) auxiliary electrode, and an Ag/AgCl reference electrode. All potentials are given versus Ag/AgCl. The experiments were carried out in acetonitrile at room temperature under argon with tetrabutylammonium hexafluorophosphate (Aldrich) as the supporting electrolyte. Under these conditions, the ferrocene/ferrocenium (Fc/Fc$^+$) couple was located at +0.44 V with a peak separation of 80 mV. Except for H-5′-NO_2phox that shows a reduction wave at −1.22 V (see above), the other ligands are not redox-active between +2.00 and −2.00 V.

Spectroelectrochemistry and Bulk Electrolysis: Butyronitrile (Acros Chimica, analytical grade) was dried with CaH_2 and freshly distilled under nitrogen. The samples were prepared under nitrogen using standard Schlenk techniques. The spectroelectrochemical experiments were conducted with saturated solutions of the complexes containing 0.3 M Bu_4NPF_6, recrystallised twice from absolute ethanol and dried in vacuo at 80 °C for 10 h. A PA4 potentiostat (EKOM, Czech Republic) was used to carry out the controlled-potential electrolyses. Bulk electrolyses were carried out in a gas-tight cell that consisted of three chambers separated at the bottom by S4 frits, with a Pt working electrode (120 mm^2 surface) in the middle, and Ag wire pseudo-reference and Pt gauze auxiliary electrodes in the lateral chambers. Chemical reduction was achieved with cobaltocene ($CoCp_2$; Aldrich), $E_{1/2}$ = −1.34 V vs. Fc/Fc$^+$. The UV/Vis spectroelectrochemical experiments at room temperature were performed with a previously described[35] Optically Transparent Thin-Layer Electrochemical (OTTLE) cell equipped with a Pt mini-grid working electrode (32 wires/cm) and quartz optical windows. The UV/Vis spectra were recorded with a software-updated Perkin−Elmer Lambda 5 spectrophotometer. X-band EPR spectra were obtained in an airtight tube cell at 77 K with a Varian Century E-104A spectrometer. EPR g values were determined relative to the 2,2′-diphenyl-1-picrylhydrazyl radical (DPPH; Aldrich) as an external "g mark" (g = 2.0037).

MO Calculations: Extended Hückel calculations were performed with the computer program CACAO (Computer Aided Composition of Molecular Orbitals).[36] The calculations were based on the X-ray diffraction data for [Mn(phox)$_3$].[12]

Catalytic Oxidation Reactions: Blank experiments were carried out in the absence of the catalyst or using manganese salts or ligands only. These experiments did not result in any epoxidation activity. Hydrogen peroxide decomposition (catalase activity) was observed with some of the reaction conditions, but systematic studies to this reaction have not been performed. − **In Methanol:** Upon stirring, 14 μmol of the catalyst was dissolved in 20 mL of MeOH at room temperature. To the resulting green solution, 14 mmol of styrene, 5.0 mmol of chlorobenzene, and 2.0 mmol of 1-methylimidazole (1-Meim) were added, followed (at t = 0 min) by 21 mmol of dihydrogen peroxide (35% in water). Except for the solution of [Mn(5′-NO_2phox)], which slowly started to turn pale yellow after t = 10 min, the colour of the solutions of the other complexes became yellowish to colourless within the first few minutes of the reactions. At t = 15 min, a sample was taken for analysis using gas chromatography with chlorobenzene as the internal standard. − **In Acetone:** Dihydrogen peroxide (21 mmol of a 35% solution in water) and 10 mL of acetone were stirred for 30 min at 0 °C. Thereafter, 14 mmol of styrene, 5.0 mmol of chlorobenzene, and 2.0 mmol of 1-Meim were added, followed by 14 μmol of the powdered catalyst (t = 0). The green solution changed to a slightly red-brown colour within the first few minutes of the reaction. After 10 min, the solution slowly turned to pale green-yellow. At t = 15 min, a sample was taken for analysis using gas chromatography with chlorobenzene as the internal standard. ***Caution!*** The mixture of acetone and dihydrogen peroxide is potentially explosive, especially under acidic conditions.[37,38] However, it can be handled safely by performing reactions on a small scale at 0 °C, using slightly alkaline conditions, as described above.

Acknowledgments

This work was carried out as part of the Innovation Oriented Research Programme on Catalysis (IOP Katalyse, no. IKA94056)

sponsored by the Netherlands Ministery of Economic Affairs. We would like to acknowledge Dr. J. G. de Vries (DSM, The Netherlands) and Dr. R. Hage (Unilever, The Netherlands) for useful discussions.

[1] M. Hoogenraad, *PhD thesis*, Leiden University, **2000**.
[2] R. Hage, *Recl. Trav. Chim. Pays-Bas.* **1996**, *115*, 385−395.
[3] T. Katsuki, in *Catalytic Asymmetric Synthesis* (Ed.: I. Ojima), Wiley-VCH, Weinheim, **2000**, p. 287.
[4] W. R. Sanderson, *Pure Appl. Chem.* **2000**, *72*, 1289.
[5] A. M. d′A. Rocha Gonsalves, M. M. Pereira, *J. Mol. Catal. A* **1996**, *113*, 209−221.
[6] K. Srinivasan, P. Michaud, J. K. Kochi, *J. Am. Chem. Soc.* **1986**, *108*, 2309−2320.
[7] M. Palucki, N. S. Finney, P. J. Pospisil, M. L. Güler, T. Ishida, E. N. Jacobsen, *J. Am. Chem. Soc.* **1998**, *120*, 948−954.
[8] H. R. Hoveyda, V. Karunaratne, S. J. Rettig, C. Orvig, *Inorg. Chem.* **1992**, *31*, 5408−5416.
[9] G. Mugesh, H. B. Singh, R. J. Butcher, *Eur. J. Inorg. Chem.* **2001**, 669−678.
[10] M. Gómez, S. Jansat, G. Muller, G. Noguera, H. Teruel, V. Moliner, E. Cerrada, M. Hursthouse, *Eur. J. Inorg. Chem.* **2001**, 1071−1076.
[11] M. Gómez-Simón, S. Jansat, G. Muller, D. Panyella, M. Font-Bardía, X.-J. Solans, *J. Chem. Soc., Dalton Trans.* **1997**, 3755−3764.
[12] M. Hoogenraad, K. Ramkisoensing, H. Kooijman, A. L. Spek, E. Bouwman, J. G. Haasnoot, J. Reedijk, *Inorg. Chim. Acta* **1998**, *279*, 217−220.
[13] M. Hoogenraad, K. Ramkisoensing, W. L. Driessen, H. Kooijman, A. L. Spek, E. Bouwman, J. G. Haasnoot, J. Reedijk, *Inorg. Chim. Acta* **2001**, *320*, 117−126.
[14] P. Basu, A. Chakravorty, *Inorg. Chem.* **1992**, *31*, 4980−4986.
[15] A. L. Spek, *PLATON, a multipurpose crystallographic tool*, Utrecht University, the Netherlands, **2000**; internet: http://www.cryst.chem.uu.nl/platon/
[16] D. H. Evans, K. M. O'Connell, R. A. Petersen, M. J. Kelly, *J. Chem. Educ.* **1983**, *60*, 290293.
[17] M. Koikawa, H. Okawa, S. Kida, *J. Chem. Soc., Dalton Trans.* **1988**, 641−645.
[18] M. R. Bermejo, A. Castiñeiras, J. C. Garcia-Monteagudo, M. Rey, A. Sousa, M. Watkinson, C. A. McAuliffe, R. G. Pritchard, R. L. Beddoes, *J. Chem. Soc., Dalton Trans.* **1996**, 2935−2945.
[19] R. I. Kureshy, N. H. Khan, S. H. R. Abdi, A. K. Bhatt, *J. Mol. Catal. A* **1996**, *110*, 33−40.
[20] J. A. Weinstein, N. N. Zheligovskaya, M. Y. Melnikov, F. Hartl, *J. Chem. Soc., Dalton Trans.* **1998**, 2459−2466.
[21] C. Mealli, D. M. Proserpio, *J. Chem. Educ.* **1990**, *67*, 399−402.
[22] M. M. Morrison, D. T. Sawyer, *Inorg. Chem.* **1978**, *17*, 333−337.
[23] K. Yamaguchi, D. T. Sawyer, *Inorg. Chem.* **1985**, *24*, 971−976.
[24] U. Auerbach, T. Weyhermüller, K. Wieghardt, B. Nuber, E. Bill, C. Butzlaff, A. X. Trautwein, *Inorg. Chem.* **1993**, *32*, 508−519.
[25] O. Schlager, K. Wieghardt, B. Nuber, *Inorg. Chem.* **1995**, *34*, 6456−6452.
[26] J. R. Pilbrow, *Transition Ion Electron Paramagnetic Resonance*, Oxford University Press, Oxford, **1990**.
[27] C. Zondervan, R. Hage, B. L. Feringa, *Chem. Commun.* **1997**, 419−420.
[28] T. Linker, *Angew. Chem. Int. Ed. Engl.* **1997**, *36*, 2060−2062.
[29] N. S. Finney, P. J. Pospisil, S. Chang, M. Palucki, R. G. Konsler, K. B. Hansen, E. N. Jacobsen, *Angew. Chem. Int. Ed. Engl.* **1997**, *36*, 1720−1723.
[30] R. I. Kureshy, N. H. Khan, S. H. R. Abdi, P. Iyer, A. K. Bhatt, *J. Mol. Catal. A* **1997**, *120*, 101−108.
[31] M. Hoogenraad, H. Kooijman, A. L. Spek, E. Bouwman, J. G. Haasnoot, J. Reedijk, manuscript in preparation.
[32] *International Tables for Crystallography*, vol. C (Ed.: A. J. C. Wilson), Kluwer Academic Publishers, Dordrecht, **1992**.
[33] P. T. Beurskens, G. Admiraal, G. Beurskens, W. P. Bosman, R. O. García-Granda, R. O. Gould, J. M. M. Smits, C. Smykalla, *The DIRDIF Program System*, Technical report of the Laboratory of Crystallography, University of Nijmegen, **1992**.
[34] S. R. Hall, G. S. D. King, J. M. Stewart, *XTAL3.4 User's manual*, Universities of Western Australia and Maryland, **1995**.
[35] M. Krejčík, M. Daněk, F. Hartl, *J. Electroanal. Chem.* **1991**, *317*, 179−187.
[36] C. Mealli, D. M. Proserpio, *CACAO version 3.3*, University of Florence, Italy, **1993**.
[37] L. Bretherick, *Handbook of Reactive Chemical Hazards*, Butterworths, London, **1975**.
[38] C. J. M. Stirling, *Chem. Br.* **1969**, *5*, 36.

Received June 21, 2001
[I01223]